*Laser and Particle Beams* (1992), *vol.* 10, *no.* 1, *pp.* 189–200
Printed in the United States of America



# Preheating of heavy-ion-beam targets by secondary particles

By M. M. BASKO
Institute of Theoretical and Experimental Physics,
B. Cheremushkinskaja 25, Moscow 117259, USSR

(Received 16 October 1990; revised received 16 January 1991)

The contribution of different sorts of secondary particles to the preheating of thermonuclear targets driven by heavy-ion beams is analyzed. Two types of illumination geometry are considered: side-on and face-on locations of the fuel with respect to the ion beam. It is shown that a substantial preheating can be expected from (1) nuclear fission fragments for the face-on fuel position and (2) $\delta$-electrons and low-$Z$ nuclear fragments for the side-on fuel location. All the X-ray and gamma photons of various origin are shown to produce a negligible fuel heating.

## 1. Introduction

An important issue in heavy-ion-beam fusion and in other possible applications of intense heavy-ion beams (Arnold & Meyer-ter-Vehn 1987) is the preheating of the thermonuclear fuel (or other sensitive target components) by secondary particles created when fast ions of the beam interact with the absorber material. As the secondary particles, one should consider electrons, photons, and nuclear fragments. Earlier, detailed calculations of the preheating of spherical DT targets by $K$- and $L$-photons and by nuclear fission fragments have been published by Anholt & Hoffmann (1985) and Beynon & Smith (1985), respectively. In distinction from their works, this paper attempts to perform a general analysis of the problem of the preheating by secondary particles generated by heavy-ion beams.

Below we assume that the fast primary ions have a high enough energy, $E_p/A_p \gtrsim 50$ MeV/amu, at which their effective charge $Z_{eff}$ practically coincides with their atomic number $Z_p$. All the possible illumination configurations are roughly divided into two categories: those in which a sensitive component (thermonuclear fuel) lies ahead of the ion beam (face-on illumination [figure 1(a)]) and those in which it is placed at the side of the beam (side-long illumination [figure 1(b)]). Specific numerical estimates are presented for the ion energy $E_p/A_p = 200$ MeV/amu, typical for the SIS-18 synchrotron in Darmstadt (Meyer-ter-Vehn 1989); in all these estimates the atomic number $Z_f$ and weight $A_f$ of the fuel are taken to be unity.

## 2. Fast electrons

The emission of fast $\delta$-electrons can be evaluated under the assumption that all the absorber electrons are initially free and motionless. Calculations are performed for the not too high values of the relativistic factor $\gamma_p \equiv (1 - \beta_p^2)^{-1/2} \lesssim 10$.

The energy of $\delta$-electrons emitted at an angle $\theta$ with respect to the primary ion velocity $\mathbf{V}_p$ in the laboratory frame is given by

 0263-0346/92 \$5.00 + .00

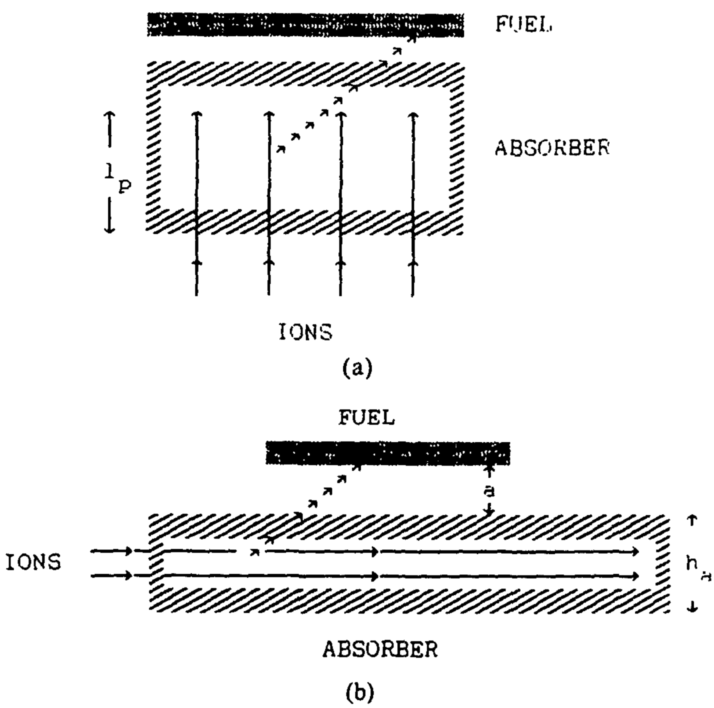


FIGURE 1. Two principal patterns of illumination by ion beams: (a) face-on illuminataion, (b) sidelong illumination.

$$E_e = 2m_eV_p^2 \frac{\gamma_p^2 \cos^2\theta}{1 + (\gamma_p^2 - 1)\sin^2\theta} = m_ec^2 \frac{2(\gamma_p^2 - 1)}{1 + \gamma_p^2 \tan^2\theta}. \tag{1}$$

Having employed the Mott formula (Akhiezer & Berestetzkii 1969) for the Coulomb scattering cross section, we obtain the following expression for the number of $\delta$-electrons emitted into a solid angle $d\Omega = 2\pi \sin\theta\, d\theta$ by one primary ion per unit mass length of its trajectory:

$$\frac{dN_e}{\rho_a dx} = \frac{r_e^2}{m_A} \frac{Z_a Z_p^2}{A_a} \frac{1}{\beta_p^4} \frac{\gamma_p^2 \tan^2\theta + \gamma_p^{-2}}{\gamma_p^2 \tan^2\theta + 1} \frac{d\Omega}{\cos^3\theta} \quad [\mathrm{cm^2\, g^{-1}\, ion^{-1}}], \tag{2}$$

where $r_e = e^2/m_ec^2$ is the electron radius; $m_A$ is the atomic mass unit; $\rho_a$, $Z_a$, and $A_a$ are the density, the atomic number, and the atomic weight of the absorber material, respectively; and $\beta_p = V_p/c$. To calculate the total number of $\delta$-electrons emitted into an energy interval $E_1 \le E_e \le E_2$, one needs to evaluate from equation (1) the corresponding angle limits $\theta_2(x) \le \theta \le \theta_1(x)$ and then to integrate equation (2) over the angle $\theta$ and the path length $x$, making use of the deceleration law (6) from which the velocity dependence $V_p = V_p(x)$ is to be found. In the nonrelativistic limit $\gamma_p - 1 \ll 1$, from equations (1) and (2) one readily obtains a well-known formula,

$$\frac{dN_e}{dx} = 2\pi n_{ea} \frac{e^4 Z_p^2}{m_e V_p^2} \left(\frac{1}{E_1} - \frac{1}{E_2}\right), \tag{3}$$

where $n_{ea} = \rho_a Z_a / m_A A_a$. As a characteristic angle interval for numerical estimates, we adopt $0° \le \theta \le 45°$, which corresponds to $\delta$-electron energies

$$2m_e c^2 \frac{\gamma_p^2 - 1}{\gamma_p^2 + 1} \le E_e \le E_{e\,\max} = 2m_e c^2(\gamma_p^2 - 1). \tag{4}$$

In the particular case of $\gamma_p = 1.215$ ($E_p/A_p = 200$ MeV/amu) each primary ion generates

$$\left.\frac{dN_e}{\rho_a\, dx}\right|_{\theta \le 45^\circ} = 1.16\, \frac{Z_a Z_p^2}{A_a} \quad [\mathrm{cm^2\, g^{-1}\, ion^{-1}}] \tag{5}$$

δ-electrons within the energy interval 200 keV $\le E_e \le$ 490 keV.

Before evaluating the preheating of the fuel by δ-electrons, we consider the problem of their escape from the absorber. The Coulomb drag force acting on a fast electron moving with velocity $v_e$ in a medium with electron density $n_{ea}$ is

$$\frac{dE_e}{dx} = -\frac{4\pi e^4}{m_e v_e^2}\, n_{ea} \ln \Lambda_e, \tag{6}$$

where the Coulomb logarithm $\ln \Lambda_e$ is given by equation (22) below. So long as $\gamma_p \lesssim (1 + 150/Z_a)^{1/2}$, radiative energy losses contribute no more than 10% to the total stopping power (Koch & Motz 1959) and can be ignored. Note that in equation (6) the path length $x$ is measured along the curved electron trajectory: being decelerated, fast electrons significantly deflect from the initial direction of their motion. For this reason the path length $l_e$ as calculated from equation (6) always exceeds the true penetration depth. The Coulomb stopping of primary ions is governed by a similar law:

$$\frac{dE_p}{dx} = -\frac{4\pi e^4 Z_p^2}{m_e V_p^2}\, n_{ea} \ln \Lambda_p. \tag{7}$$

Typically, for projectile ion energies of interest here the difference between the electron $\ln \Lambda_e$ and ion $\ln \Lambda_p$ Coulomb logarithms does not exceed 10–20% (Ahlen 1980), and we can neglect this difference for the moment in order to obtain from equations (6) and (7) the following relationship between the path length of the most energetic δ-electrons and that of primary ions:

$$\frac{l_e}{l_p} < \frac{E_{e\,\max}}{E_p}\, \frac{v_{e\,\max}^2}{V_p^2}\, Z_p^2 = 8\, \frac{\gamma_p^4(\gamma_p + 1)}{(2\gamma_p^2 - 1)^2}\, \frac{m_e}{m_A}\, \frac{Z_p^2}{A_p}. \tag{8}$$

For $\gamma_p < 10$ we have $l_e/l_p < 0.4$. From this we conclude that in targets with the face-on illumination pattern [figure 1(a)] none of the δ-electrons can reach beyond the absorber and contribute to the preheating of the fuel.

Under the side-long illumination [figure 1(b)] a substantial fraction of the δ-electrons can escape the absorber when its thickness $h_a$ is much less than the Coulomb path length $l_p$ of the primary ions. In this case it would be expedient to evaluate the thickness $h_s$ of a shield that could stop all the δ-electrons born in the absorber. For this we assume that the shield and the absorber are of the same material and that the path length $l_e$ of electrons with energy $E_e$ obeys the law

$$l_e = l_{e\,\max} \left( \frac{E_e}{E_{e\,\max}} \right)^m, \tag{9}$$

where $l_{e\,\max}$ is the path length of electrons with the maximum energy $E_{e\,\max} = 2m_e c^2(\gamma_p^2 - 1)$ and the exponent $m$ lies in the interval $1 < m < 2$. From equations (1), (8), and (9) one readily obtains

$$h_s = \lambda\, \frac{m_e}{m_A}\, \frac{Z_p^2}{A_p}\, l_p, \tag{10}$$

where

$$\lambda = 8\,\frac{\gamma_p^4(\gamma_p+1)}{(2\gamma_p^2-1)^2}\,\max_\theta\left(\frac{(\sin\theta)(\cos\theta)^{2m'}}{[1+(\gamma_p^2-1)\sin^2\theta]^{m}}\right). \tag{11}$$

The angle of deepest penetration $\theta_m$, at which the maximum in equation (11) occurs, in the nonrelativistic limit is equal to 30° (±3°) and monotonically decreases with increasing $\gamma_p$. For $\gamma_p = 1$ the coefficient $\lambda \approx 5$, for $\gamma_p = 1.2$ it falls to $\lambda \approx 3$, and then, at $\gamma_p \gtrsim 5$, it approaches an almost constant value of $\lambda \approx 1$. Specifically, with irradiation by heavy ions with $Z_p = 80$ and $E_p/A_p = 200$ MeV/amu, a screen with a thickness $\simeq 5\%$ of the ion Coulomb range $l_p$ will absorb all the $\delta$-electrons. In cases in which no such screen is present and the transverse dimensions of the absorber are such that $h_a < h_s$, a considerable fraction of the fast $\delta$-electrons will be able to escape the absorber and to heat up the fuel.

We evaluate the preheating of the fuel by fast electrons under the assumption that the whole target is transparent for them. Consider a fuel element at a distance $a$ from the fast-ion trajectory [see figure 1(b)]. Then the specific energy release due to $\delta$-electrons emitted by one primary ion into the angle interval $\theta_1 \le \theta \le \theta_2$ is

$$q_e = \frac{r_e^2}{a}\int_{\theta_1}^{\theta_2}\frac{\gamma_p^2\tan^2\theta+\gamma_p^{-2}}{\gamma_p^2\tan^2\theta+1}\,\frac{n_{ea}Z_p^2}{\beta_p^4}\left|\left(\frac{dE_e}{\rho\,dx}\right)_f\right|\frac{d\theta}{\cos^3\theta}\quad\left[\frac{\text{erg}}{\text{g}\cdot\text{ion}}\right]. \tag{12}$$

Here $[dE_e/\rho\,dx]_f$ is the fuel stopping power for electrons with energy $E_e$, which can be evaluated from equation (6) after one substitutes $n_{ef}$ for $n_{ea}$. Generally, $n_{ea}$ and $\beta_p$ in equation (12) depend on $\theta$ via the coordinate $x = -a\cot\theta$ along the ion path. Here and below, we estimate the heating of the fuel under the simplifying assumption $l_p \gg a$ when the variation of $\beta_p$ due to ion deceleration can be ignored. Neglecting also the dependence of the Coulomb logarithm $\ln\Lambda_e$ on the electron energy $E_e$, from equations (1), (6), and (12) we obtain

$$q_e = \pi\,\frac{r_e^4 m_e c^2}{m_A^2}\,\frac{\rho_a}{a}\,\frac{Z_a Z_f}{A_a A_f}\,Z_p^2\,\frac{\ln\Lambda_e}{\beta_p^6}\,I_e, \tag{13}$$

where

$$I_e = \int_{\theta_1}^{\theta_2}\frac{1+\beta_p^2+\tan^2\theta}{\cos\theta}\,\frac{\gamma_p^2\tan^2\theta+\gamma_p^{-2}}{\gamma_p^2\tan^2\theta+1}\,d\theta \tag{14}$$

is a weak function of the primary ion energy.

As a specific example, consider a beam of $N_p = 10^{15}$ bismuth ions at 200 MeV/amu (the total energy in the beam is 6.7 MJ) propagating through a thin beryllium wire. Having adopted $\theta_1 = 20°$ and $\theta_2 = 45°$ as lower and upper integration limits in equation (14)—which correspond to $\delta$-electron energies 196 keV $\le E_e \le$ 406 keV and to the value of $I_e$ = 1.4—we obtain the preheating intensity of $q_e = 0.07$ erg g$^{-1}$ ion$^{-1}$ for a hydrogen element located at $a = 0.2$ cm from the ion trajectory [figure 1(b)]. The total specific energy release is then $q_e N_p = 7 \times 10^{13}$ ergs/g, which corresponds to the temperature rise of $\Delta T_f = 24$ eV. Thus, with a side-long illumination by heavy-ion beams, the fast $\delta$-electrons can, under certain conditions, cause a substantial preheating of the thermonuclear fuel.

Note that, having assumed that $Z_{eff} = Z_p$ for projectile ions, we actually overestimate the influence of $\delta$-electrons at lower projectile energies, $E_p/A_p < 50$ MeV/amu. Hence, if we relax this simplifying assumption, we will only strengthen the above conclusion that $\delta$-electrons cannot reach the fuel in the face-on geometry and the conclusion of Sec. 3 that bremsstrahlung photons contribute only negligibly to the fuel preheating. As regards the side-on fuel location, the above estimate is of course very crude and indicates only that the preheating by $\delta$-electrons may be important. It means that for any specific target design of this type one must evaluate the preheating by $\delta$-electrons under the more rigorous Fokker-Planck formalism and to relax, if necessary, the simplifying assumptions used in this paper. Another such assumption, $V_p \gg v_e$ (here $v_e$ is the typical velocity of absorber electrons), usually holds over the major portion of the projectile trajectory along which most of the secondary particles originate, if only the initial energy of fast ions falls in the range ($E_p/A_p > 20$ MeV/amu) that is of primary interest for heavy-ion-driven fusion.

## 3. X-ray and gamma photons

The interaction of energetic heavy ions with matter is accompanied by the generation of a multicomponent hard-X-ray spectrum (Anholt *et al.* 1986). Below we examine the most important of its components and demonstrate that, irrespective of the illumination geometry, none of them can cause any significant preheating of the thermonuclear fuel.

### 3.1 *Secondary bremsstrahlung*

When fast $\delta$-electrons are being Coulomb scattered by the absorber nuclei, they emit hard bremsstrahlung photons. Such photons penetrate much deeper than the parent $\delta$-electrons: for example, the path length of 100-keV electrons in beryllium is ~0.02 g/cm$^2$, while that of 100-keV photons is ~6 g/cm$^2$. We evaluate the generation of secondary bremsstrahlung photons under the assumption that all the $\delta$-electrons are stopped in the absorber.

We take the bremsstrahlung cross section in the form (Koch & Motz 1959)

$$\frac{d\sigma_{\text{brem}}}{d(\hbar\omega)} = \frac{16}{3}\alpha r_e^2 Z_a^2 \frac{1}{\beta_e^2}\frac{\phi(\bar{\omega}, \epsilon_e, Z_a)}{\hbar\omega}, \tag{15}$$

where $v_e = \beta_e c$ is the electron velocity and $\alpha = e^2/\hbar c = 1/137$. In the Kramers approximation, $\phi = \pi/\sqrt{3}$. We make use of the nonrelativistic Born approximation with the Coulomb correction by Elwert (Koch & Motz 1959) when

$$\phi(\bar{\omega}, \epsilon_e, Z_a) = \frac{\beta_e[1 - \exp(-2\pi\alpha Z_a/\beta_e)]}{\beta_f[1 - \exp(-2\pi\alpha Z_a/\beta_f)]} \ln\left(\frac{\beta_e + \beta_f}{\beta_e - \beta_f}\right). \tag{16}$$

Here

$$\beta_e^2 = \frac{\epsilon_e(2 + \epsilon_e)}{(1 + \epsilon_e)^2}, \qquad \beta_f^2 = \frac{(\epsilon_e - \bar{\omega})(2 + \epsilon_e - \bar{\omega})}{(1 + \epsilon_e - \bar{\omega})^2},$$
$$\epsilon_e = \frac{E_e}{m_e c^2}, \qquad \bar{\omega} = \frac{\hbar\omega}{m_e c^2}. \tag{17}$$

In the worst case, when $\epsilon_e \sim 1$, approximation (16) may underestimate the bremsstrahlung cross section by a factor of ~2 (Koch & Motz 1959). Assuming that the stopping of electrons with energy $E_e$ is primarily due to the ionization losses and governed by equation (6), the total number of bremsstrahlung photons emitted into a frequency interval $(\omega, \omega + d\omega)$ over the entire electron path length can be estimated as

$$\frac{dN_{\text{brem}}}{d(\hbar\omega)} = \frac{4}{3\pi}\frac{\alpha Z_a}{\hbar\omega}\int_{\bar{\omega}}^{\epsilon_e} \frac{\phi(\bar{\omega}, \epsilon_e', Z_a)}{\ln[\Lambda_e(\epsilon_e')]}\, d\epsilon_e'. \tag{18}$$

From equations (2) and (18) we obtain the following expression for the number of secondary bremsstrahlung photons emitted by a single primary ion per unit of its path length:

$$\frac{dN_{ba}}{\rho_a\,dx\,d(\hbar\omega)} = \frac{8\alpha}{3}\,\frac{r_e^2}{m_A}\,\frac{Z_a^2 Z_p^2}{A_a}\,\frac{\Phi_a(\bar{\omega}, \gamma_p, Z_a)}{\beta_p^2 \hbar\omega} \quad \left[\frac{\text{cm}^2}{\text{g}\cdot\text{ion}}\right]. \tag{19}$$

A slowly varying function $\Phi_a$ is defined by

$$\Phi_a = \frac{1}{2\beta_p^2}\int_1^{\xi_1} \frac{\gamma_p^2(\xi - 1) + \gamma_p^{-2}}{\gamma_p^2(\xi - 1) + 1}\left(\int_{\bar{\omega}}^{\epsilon_e(\xi)} \frac{\phi(\bar{\omega}, \epsilon_e', Z_a)}{\ln[\Lambda_e(\epsilon_e')]}\,d\epsilon_e'\right)d\xi, \tag{20}$$

where

$$\xi_1 = \beta_p^2(1 + 2/\bar{\omega}), \qquad \epsilon_e(\xi) = \frac{2\beta_p^2}{\xi - \beta_p^2}. \tag{21}$$

The behavior of $\Phi_a(\omega)$ for some $\gamma_p$ and $Z_a$ is illustrated in figure 2. For the Coulomb logarithm $\ln \Lambda_e$ the formula

$$\ln \Lambda_e = \ln\left(\frac{\epsilon_e(1 + \epsilon_e/2)^{1/2}}{I(Z_a)/m_e c^2}\right), \tag{22}$$

approximating a more accurate expression by Rohrlich & Carlson (1954), was used. The effective ionization potentials $I(4) = 64$ eV and $I(79) = 770$ eV were taken from Ahlen (1980). The total number of photons emitted into a finite frequency interval $\omega_1 \leq \omega \leq \omega_2$ from the unit path length can, by analogy with equation (5), be expressed as

$$\frac{dN_{ba}}{\rho_a\,dx} = \Omega_{12}\,\frac{Z_a^2 Z_p^2}{A_a} \quad [\text{cm}^2\,\text{g}^{-1}\,\text{ion}^{-1}]. \tag{23}$$

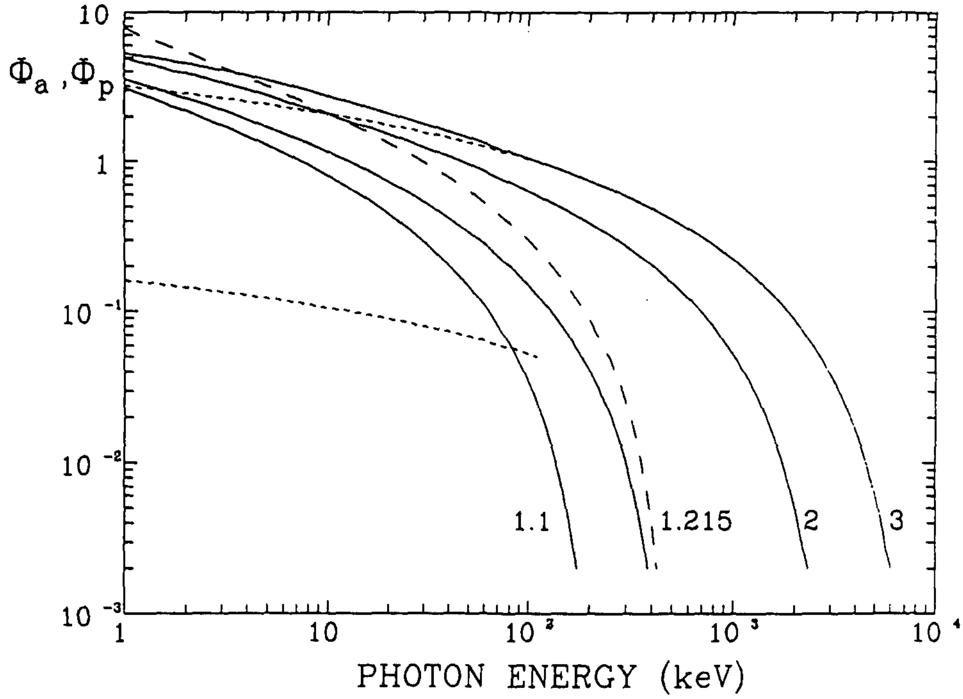


FIGURE 2. Solid curves: plots of $\Phi_a(\omega, \gamma_p, Z_a)$ defined in equation (20) for $Z_a = 4$ and $\gamma_p = 1.1$, 1.215, 2, and 3. Dashed curve: plot of $\Phi_a(\omega, \gamma_p, Z_a)$ for $\gamma_p = 1.215$ and $Z_a = 79$. Dotted curves: plots of $\Phi_p(\omega, \gamma_p, Z_a, Z_p)$ defined in equation (28) for $\gamma_p = 1.215$, $Z_p = 83$, $Z_a = 4$ (upper curve), and $Z_a = 79$ (lower curve).

TABLE 1. Values of coefficient $\Omega_{12}$ ($cm^2/g$) from equation (23) for $\gamma_p = 1.215$

| | $\hbar\omega_1$-$\hbar\omega_2$ (keV) | | | | |
|---|---|---|---|---|---|
| | 10–20 | 20–50 | 50–100 | 100–200 | 200–500 |
| $Z_a = 4$ | $1.9 \times 10^{-3}$ | $1.4 \times 10^{-3}$ | $4.8 \times 10^{-4}$ | $1.8 \times 10^{-4}$ | $3.2 \times 10^{-5}$ |
| $Z_a = 79$ | $3.4 \times 10^{-3}$ | $2.5 \times 10^{-3}$ | $9.1 \times 10^{-4}$ | $3.7 \times 10^{-4}$ | $7.5 \times 10^{-5}$ |

The values of coefficient $\Omega_{12} = \Omega_{12}(\omega_1, \omega_2, \gamma_p, Z_a)$ for the primary ion energy $E_p/A_p = 200$ MeV/amu are given in Table 1.

Hard photons with $\hbar\omega \gtrsim 10$ keV heat up the hydrogen by means of the Compton scattering, for which the mean energy transfer to an electron at rest is given by

$$\langle \hbar(\omega - \omega')\sigma_c \rangle = \hbar \int_0^{\omega} (\omega - \omega') \frac{d\sigma_c}{d\omega'} = \pi r_e^2 m_e c^2 \Delta_c(\bar{\omega}), \tag{24}$$

where (Akhiezer & Berestetzkii 1969)

$$\Delta_c(\bar{\omega}) = \left(1 - \frac{2}{\bar{\omega}} - \frac{3}{\bar{\omega}^2}\right)\ln(1 + 2\bar{\omega}) + \frac{6}{\bar{\omega}} - 2\,\frac{1 + 3\bar{\omega} + \bar{\omega}^2}{(1 + 2\bar{\omega})^2} - \frac{8}{3}\,\frac{\bar{\omega}^3}{(1 + 2\bar{\omega})^3}$$
$$= \frac{8}{3}\bar{\omega}^2\left(1 - \frac{21}{5}\bar{\omega} + \ldots\right), \quad \bar{\omega} \ll 1. \tag{25}$$

Assuming that all the $\delta$-electrons are stopped in the absorber while the bremsstrahlung photons escape freely with an isotropic angular distribution, we obtain the following estimate for the preheating of a fuel element at a distance $a$ from the ion trajectory:

$$q_{ba} = \frac{2\pi}{3}\,\alpha\,\frac{r_e^4 m_e c^2}{m_A^2}\,\frac{\rho_a}{a}\,\frac{Z_a^2 Z_f}{A_a A_f}\,\frac{Z_p^2}{\beta_p^2}\,I_{ba}, \tag{26}$$

where

$$I_{ba} = \int_0^{2(\gamma_p^2 - 1)} \Delta_c(\bar{\omega})\Phi_a(\bar{\omega}, \gamma_p, Z_a)\,\frac{d\bar{\omega}}{\bar{\omega}}. \tag{27}$$

Table 2 lists the values of $I_{ba}$ for four values of $\gamma_p$. Note that the main contribution to the integral in equation (27) comes from relatively high frequencies $\bar{\omega} \sim (0.2\text{-}1)(\gamma_p^2 - 1)$, for which one can safely ignore the photoelectric absorption by hydrogen atoms.

In the specific case of $N_p = 10^{15}$, $Z_p = 83$, $E_p/A_p = 200$ MeV/amu, $Z_a = 4$, and $a = 0.2$ cm we obtain $q_{ba}N_p = 1.8 \times 10^8$ ergs/g, which corresponds to the fuel temperature rise of

TABLE 2. Values of $I_{ba}$ from equation (27)

| | $\gamma_p$ | | | |
|---|---|---|---|---|
| | 1.1 | 1.215 | 2 | 3 |
| $Z_a = 4$ | $5.6 \times 10^{-3}$ | $1.8 \times 10^{-2}$ | 0.167 | 0.49 |
| $Z_a = 79$ | $1.2 \times 10^{-2}$ | $3.6 \times 10^{-2}$ | 0.264 | 0.70 |

$\Delta T_f \simeq 6 \times 10^{-5}$ eV. For the face-on illumination [figure 1(a)] one finds approximately equally low values of the preheating by the secondary bremsstrahlung photons, provided that the irradiation does not exceed $10^{16}$ ions/cm$^2$.

### 3.2 *Primary bremsstrahlung*

The primary bremsstrahlung originates from the Coulomb scattering of the absorber electrons off the primary ions; i.e, it accompanies the emission of $\delta$-electrons. In general, the spectrum of this X-ray component is to be found via the Lorentz transformation of the bremsstrahlung spectrum from the comoving frame (Anholt *et al.* 1986). In the relativistic case $\gamma_p \gtrsim 2$ the high-energy cutoff of the primary bremsstrahlung $\bar{\omega}_{pm} = (1 - \gamma_p^{-1})(1 - \beta_p \cos\theta)^{-1}$ strongly depends on the emission angle $\theta$; but for any $\theta$ it is below the edge of the secondary bremsstrahlung $\bar{\omega}_{am} = 2(\gamma_p^2 - 1)$. For the goals of this paper, however, it is quite sufficient to restrict ourselves to a nonrelativistic estimate, when the emission of the primary bremsstrahlung can be described by equation (19) with $\Phi_a$ replaced by

$$\Phi_p(\bar{\omega}, \gamma_p, Z_a, Z_p) = \frac{2}{Z_a}\, \phi(\bar{\omega}, \gamma_p - 1, Z_p). \tag{28}$$

The behavior of $\Phi_p(\omega)$ for $\gamma_p = 1.215$, $Z_p = 83$, and the two values of $Z_a = 4$ and 79 is shown in figure 2 as the dotted curves. From this figure it is seen that for $Z_a \lesssim 10$ the emission of the primary bremsstrahlung can be a factor of 2–5 more intensive than that of the secondary bremsstrahlung, while for $Z_a \gtrsim 20$ the secondary bremsstrahlung dominates. It is quite clear also that even in the worst case the preheating by the primary bremsstrahlung $q_{bp}$ cannot exceed $q_{ba}$ by more than a factor of ~2–3, which, as shown in Sec. 3.1, is still negligibly small.

### 3.3 *Atomic K- and R-photons*

Besides the continuum primary and secondary bremsstrahlung emission, heavy-ion beams generate *K*-lines of the absorber and beam atoms as well as an *R*-line originating from the radiative recombination onto the vacant *K*-shell of the beam ions (Anholt *et al.* 1986). When a beam of fast ions with $Z_p \simeq 80$–90 irradiates an absorber with $Z_a \simeq 80$–90, the most important will be the absorber *K*-photons. Their contribution to the thermonuclear fuel preheating in the case of face-on illumination has been meticulously calculated by Anholt & Hoffmann (1985). At $E_p/A_p \gtrsim 100$ MeV/amu the cross section for *K*-line excitation in the absorber atoms, $\sigma_{Ka}$, is practically independent of the primary ion energy $E_p$, and for $Z_p \approx Z_a \approx 80$ it is $\sigma_{Ka} \approx 6 \times 10^{-20}$ cm$^2$ (Anholt & Hoffmann 1985). To a first approximation, we can assume that $\sigma_{Ka} \propto (Z_p/Z_a)^2$ (Anholt *et al.* 1984). Then, for the rate of the absorber *K*-photon generation, we obtain

$$\frac{dN_K}{\rho_a\, dx} = \frac{\sigma_{Ka}}{m_A A_a} \approx 3.6 \times 10^4\, \frac{Z_p^2}{Z_a^2 A_a} \quad \left[\frac{\text{cm}^2}{\text{g}\cdot\text{ion}}\right]. \tag{29}$$

A comparison of equations (23) and (29) reveals that, in an absorber with $Z_a \simeq 80$, about as many *K*-photons will be generated as the number of the secondary bremsstrahlung photons in the frequency range $\Delta\omega \sim \omega_K$. The heating of a fuel element at a distance $a$ from the ion path is given by

$$q_K = \frac{\pi}{4}\, \frac{r_e^2 m_e c^2}{m_A}\, \frac{Z_f}{A_f}\, \Delta_c(\bar{\omega}_K)\, \frac{\rho_a}{a} \left(\frac{dN_K}{\rho_a\, dx}\right) \quad \left[\frac{\text{erg}}{\text{g}\cdot\text{ion}}\right]. \tag{30}$$

Although the number of $K$-photons increases with decreasing $Z_a$, the fuel heating $q_K$ will nevertheless decrease because of the decreasing $K$-line frequency $\omega_K \propto Z_a^2$. In addition, with lower $Z_a$ a smaller portion of $K$-photons will escape the absorber, owing to the steeply growing photoelectric cross section. All in all, the maximum fuel preheating by $K$-photons should be expected for $Z_p = Z_a \simeq 80$–$90$; with $a = 0.2$ cm, $\rho_a = 20$ g/cm$^2$, and $N_p = 10^{15}$ it may amount to $q_K N_p \simeq 2 \times 10^{10}$ ergs/g, which corresponds to the temperature increase of $\Delta T_f \simeq 0.007$ eV. Recall that equation (30) has been derived under the assumption $l_p \gg a$, which, for the case being discussed, requires that $\gamma_p \gtrsim 2$. If $\gamma_p \lesssim 1.3$, the range of bismuth ions in gold $l_p \lesssim 0.2$ cm and the value of $\Delta T_f$ will be at least a factor of 2 lower.

For the same reason, for which the heating by $K$-photons drops with decreasing $Z_a$, the heating by $L$-photons will be always less than that by $K$-photons. At not too high velocities $V_p$, when the primary ions have three or more bound electrons, the $K$-photons of the beam ions might seem to be of importance. However, for $Z_a \simeq Z_p$, the cross section for excitation of these photons, $\sigma_{Kp}$, is at least a few times less than $\sigma_{Ka}$ (Anholt *et al.* 1984) because of the atomic screening of exciting charges $Z_a$, while for smaller $Z_a$, $\sigma_{Kp}$ drops as $Z_a^2$. As a result, the preheating by the beam $K$-photons will be always less than the preheating by the absorber $K$-photons for $Z_a \simeq Z_p \simeq 80$–$90$.

At high enough beam velocities, when fast primary ions have vacancies in the $K$-shell, one must account for $R$-photons originating from the radiative recombination to these vacancies. For the rate of $R$-photon generation we have

$$\frac{dN_R}{\rho_a\,dx} = \frac{Z_a}{A_a}\frac{\sigma_{rp}}{m_A} = \frac{16\pi}{3\sqrt{3}}\alpha^3 \frac{r_e^2}{m_A}\frac{Z_a Z_p^4}{A_a}\frac{1}{\beta_p^2 \bar{\omega}_R}, \tag{31}$$

where

$$\bar{\omega}_R = \gamma_p - 1 + \tfrac{1}{2}\alpha^2 Z_p^2 \tag{32}$$

is the frequency of $R$-photons in the comoving frame (transformation to the laboratory frame changes the frequency and the angular distribution of $R$-photons but not their total number). In equation (31) the principle of detailed balance has been used to express the recombination cross section $\sigma_{rp}$ in terms of the photoionization one, with the Kramers approximation for the latter (Zel'dovich & Raizer 1967). The fuel heating by $R$-photons, $q_R$, can be evaluated from equation (30) with index $K$ replaced by $R$. In particular, for the above-chosen example of $Z_a = 4$, $Z_p = 83$, $\gamma_p = 1.215$, $a = 0.2$ cm, and $N_p = 10^{15}$ we obtain $q_R N_p \simeq 1.2 \times 10^9$ ergs/g and $\Delta T_f \simeq 4 \times 10^{-4}$ eV. Note that, according to equations (31) and (32), the main characteristics of the $R$-emission are practically independent of the absorber material. Having compared equations (20), (28), (29), and (31), we conclude that the X-ray preheating of the thermonuclear fuel is dominated by the absorber $K$-photons for $Z_a \simeq 80$–$90$ and by the beam $R$-photons for $Z_a \lesssim 10$.

### 3.4 *Nuclear gamma photons*

In general, one can only very roughly point out the characteristics of $\gamma$-photons created in the beam–absorber nuclear collisions. The typical energy of $\gamma$-photons should be from ~100 keV to a few MeV, and the typical summed cross section of creation should be $\sigma_\gamma \simeq 1$ b. Hence one can expect

$$\frac{dN_\gamma}{\rho_a\,dx} = \frac{\sigma_\gamma}{m_A A_a} \simeq A_a^{-1} \quad \left[\frac{\text{cm}^2}{\text{g}\cdot\text{ion}}\right] \tag{33}$$

$\gamma$-photons of nuclear origin per unit path length of the primary ion. The heating of the fuel can be estimated from equation (30), in which index $K$ should be replaced by $\gamma$. Taking

$\Delta_c = 1$ (which corresponds to photon energies $\hbar\omega \simeq$ 1–2 MeV), $A_a = 9$, $\rho_a = 1.9$ g/cm$^3$, $a = 0.2$ cm, and $N_p = 10^{15}$, we obtain $q_\gamma N_p \simeq 3 \times 10^7$ ergs/g and $\Delta T_f \simeq 10^{-5}$ eV.

## 4. Nuclear fragments

Nuclear collisions of energetic ($E_p/A_p \gtrsim 50$ MeV/amu) heavy ions with the absorber nuclei will produce a wide spectrum of nuclear fragments with various $Z_{fr}$, $A_{fr}$, energies $E_{fr}$, and escape directions. In targets with the face-on illumination pattern the most harmful seem to be heavy fission fragments preserving the primary beam velocity $\mathbf{V}_p$. From equation (7) one readily ascertains that the Coulomb range of such fragments with $Z_{fr} \simeq Z_p/2$ and $A_{fr} \simeq A_p/2$ is about twice that of the primary ions. The effect of the preheating by fission fragments on the implosion of a specific spherical DT target irradiated by uranium ions with $E_p = 10$ GeV was calculated by Beynon & Smith (1985). Below we present a more general, though less accurate, estimate that agrees quite well with the results of Beynon & Smith (1985).

The cross section of fission into two heavy fragments can be as high as 50% of the total nuclear cross section $\sigma_{n\,\mathrm{tot}}$ (Jain *et al.* 1984), for which the simple formula of Bradt & Peters (1950) can be used:

$$\sigma_{n\,\mathrm{tot}} = \pi(0.145 A_p^{1/3} + 0.145 A_a^{1/3} - 0.17)^2 \quad [\mathrm{b}]. \tag{34}$$

Assuming for simplicity that in every fission event two identical fragments with $Z_{fr} = Z_p/2$ are created and that they leave the absorber with the parent ion velocity $\mathbf{V}_p$, we derive the following expression for the fuel preheating in the case of face-on illumination:

$$\begin{aligned} q_{fr} N_p &= \frac{dN_p}{dS}\,\frac{\sigma_{n\,\mathrm{tot}}\rho_a}{m_A A_a} \int_0^{l_p} \left(\pi \frac{e^4 Z_p^2}{m_e V_p^2}\,\frac{Z_f}{m_A A_f} \ln \Lambda_{fr}\right) dx \\ &= \frac{1}{4}\,\frac{\sigma_{n\,\mathrm{tot}} E_p}{m_A Z_a}\,\frac{Z_f}{A_f}\,\frac{\langle \ln \Lambda_{fr}\rangle}{\langle \ln \Lambda_p \rangle}\,\frac{dN_p}{dS}. \end{aligned} \tag{35}$$

Here we have made use of the fact that, apart from the Coulomb logarithms and some constant factors, the fuel stopping power for fragments (the integrand) coincides with the absorber stopping power for primary ions; $dN_p/dS$ is the number of primary ions impinging on the unit surface area of the absorber. Note that, according to equation (35), for a fixed energy release per unit surface area $E_p dN_p/dS$ the preheating by fission fragments depends essentially on the beam and absorber nucleus species only. For $E_p dN_p/dS = 10$ MJ/cm$^2$, $Z_p = 83$, and $Z_a = 4$, equation (35) gives $q_{fr} N_p \simeq 10^{13}$ ergs/g and $\Delta T_f = 3$ eV.

In targets with the side-long illumination a major contribution to the fuel preheating is to be expected from the light products of the nuclear fragmentation, $Z_{fr} \lesssim 10$, that are emitted in transverse directions at energies $E_{fr}/A_{fr} \sim 10$ MeV/amu (Warwick *et al.* 1983) and have the ranges $\rho_a l_{fr} \gtrsim 0.03$–$0.1$ g/cm$^2$. In general, only a rough estimate of the preheating $q_{fr}$ can be given. Let $d^2\sigma_{fr}/dE_{fr}\,d\Omega$ be the double differential cross section for creation of a fragment ($Z_{fr}$, $A_{fr}$) with an energy $E_{fr}$ emitted at an angle $\theta$ in the laboratory frame. Under the assumption that the target is transparent to the nuclear fragments, the heating of a fuel element at a distance $a$ from the primary ion trajectory is

$$\begin{aligned} q_{fr} &= \frac{\rho_a}{a m_A A_a} \sum_{fr} \iint \frac{d^2\sigma_{fr}}{dE_{fr}\,d\Omega} \left| \left(\frac{dE_{fr}}{\rho\,dx}\right)_f \right| d\theta\, dE_{fr} \\ &= \frac{2\pi e^4}{a m_e m_A}\,\frac{\rho_a}{A_a}\,\frac{Z_f}{A_f} \sum_{fr} \iint \frac{d^2\sigma_{fr}}{dE_{fr}\,d\Omega}\, Z_{fr}^2 A_{fr} \ln \Lambda_{fr}\, d\theta\, \frac{dE_{fr}}{E_{fr}}. \end{aligned} \tag{36}$$

As a reasonable estimate for the double differential cross section the value $d^2\sigma_{fr}/dE_{fr}d\Omega =$ 1 mb/(MeV·sr) can be adopted (Warwick *et al.* 1983). Summing over the interval $1 \leq Z_{fr} \leq 10$ and taking $\Delta \ln E_{fr} = 1$ and $\Delta\theta = \pi$ as characteristic energy and angle intervals, respectively, from equation (36) we obtain $q_{fr}N_p \simeq 2 \times 10^{13}$ ergs/g and $\Delta T_f \simeq 7$ eV for the values of $N_p = 10^{15}$, $a = 0.2$ cm, $A_a = 9$, and $\rho_a \simeq 1.9$ g/cm$^3$. Note that the estimate (36) is rather crude. To obtain a better estimate, one needs more detailed information on the differential cross section $d^2\sigma_{fr}/dE_{fr}d\Omega$ for every fragment species and, having specified the target setup, must account for the energy losses by the fragments on their way to the fuel.

A certain contribution to the fuel preheating might be expected from nuclear collisions in which the absorber nuclei are scattered off the projectile ions unshattered (either in the ground state or in one of the excited states). But, to be able to reach the fuel, such absorber nuclei must acquire high enough energy, $E_a/A_a \gtrsim 10$ MeV/amu, which corresponds to a rather high transferred momentum, $\Delta P_a \gtrsim 100A_a$ MeV/$c$. From experiments with high-energy protons (Bertini *et al.* 1973) it is known that the scattering cross sections for events with such high momentum transfer are extremely low, many orders of magnitude less than 1 mb/sr (in this type of collision the cross sections for high-$Z$ projectiles may differ from those for protons with the same momentum transfer by only an insignificant geometric factor $\sim A_p^{2/3}$). Thus the preheating due to the scattering of even low-$Z$ absorber nuclei will be orders of magnitude less than that given by the above estimates (35) and (36). And only when the absorber material contains hydrogen does this effect probably need to be taken into account.

## 5. Basic conclusions

Irradiation of targets by intense beams of heavy ions will be accompanied by generation of a variety of secondary particles—$\delta$-electrons, hard electromagnetic quanta, and nuclear fragments. The most dangerous from the viewpoint of the thermonuclear fuel preheating will be the charged secondary particles with the shortest Coulomb ranges that still escape the absorber and reach the fuel. Simple estimates show that the fuel preheating by secondary and tertiary X-ray and gamma photons will probably never exceed $\Delta T_f \simeq 0.01$ eV.

The fuel preheating by fast $\delta$-electrons can occur only in targets with the side-long illumination geometry (figure 1(b)], when the fuel is at the side of the ion beam. If no precautionary measures are taken, the preheating by $\delta$-electrons from an ~10-MJ ion beam can raise the fuel temperature to $T_f \sim 10$–$30$ eV.

The effect of nuclear fragments may be significant for any illumination pattern. Under the face-on illumination the main contribution to the preheating is to be expected from heavy fission fragments with $Z_{fr} \sim Z_p/2$, while under the side-long illumination light nuclei with $Z_{fr} \lesssim 10$ born in peripheral encounters and multifragmentation reactions may produce a considerable effect. In either case the preheating of the thermonuclear fuel can reach $\Delta T_f \sim 1$–$3$ eV.

## Acknowledgments

The author acknowledges very helpful and stimulating discussions with M. D. Churazov and B. Yu. Sharkov.

## REFERENCES

AHLEN, S. P. 1980 *Rev. Mod. Phys.* 52, 121.

AKHIEZER, A. I. & BERESTETZKII, V. B. 1969 *Kvantovaja elektrodinamika* (*Quantum Electrodynamics*) (Nauka, Moscow).

ANHOLT, R. & HOFFMANN, D. H. H. 1985 *Nucl. Instrum. Methods Phys. Res. A* **240**, 567.

ANHOLT, R. *et al.* 1984 *Phys. Rev. A* **30**, 2234.

ANHOLT, R. *et al.* 1986 *Phys. Rev. A* **33**, 2270.

ARNOLD, R. C. & MEYER-TER-VEHN, J. 1987 *Rep. Prog. Phys.* **50**, 559.

BERTINI, R. *et al.* 1973 *Phys. Lett.* **45B**, 119.

BEYNON, T. D. & SMITH, E. H. 1985 *Phys. Lett.* **109A**, 163.

BRADT, H. L. & PETERS, B. 1950 *Phys. Rev.* **77**, 54.

JAIN, P. L. *et al.* 1984 *Phys. Rev. Lett.* **52**, 1763.

KOCH, H. W. & MOTZ, J. W. 1959 *Rev. Mod. Phys.* **31**, 920.

MEYER-TER-VEHN, J. 1989 *Nucl. Instrum. Methods Phys. Res. A* **278**, 25.

ROHRLICH, F. & CARLSON, B. C. 1954 *Phys. Rev.* **93**, 38.

WARWICK, A. I. *et al.* 1983 *Phys. Rev. C* **27**, 1083.

ZEL'DOVICH, YA. B. & RAIZER, YU. P. 1967 *Physics of Shock Waves and High-Temperature Hydrodynamic Phenomena* (Academic, New York).